

Guanyl Nucleotide Exchange Factor *Sql2* and *Ras2* Regulate Filamentous Growth in *Ustilago maydis*

Philip Müller, Jörg D. Katzenberger,† Gabriel Loubradou,‡ and Regine Kahmann*

Max Planck Institute for Terrestrial Microbiology, D-35043 Marburg, and Institute for Genetics and Microbiology, University of Munich, D-80638 Munich, Germany

Received 23 September 2002/Accepted 22 February 2003

The cyclic AMP (cAMP)-signaling pathway regulates cell morphology and plays a crucial role during pathogenic development of the plant-pathogenic fungus *Ustilago maydis*. Strains lacking components of this signaling pathway, such as the α -subunit Gpa3 or the adenylyl cyclase Uac1, are nonpathogenic and grow filamentously. On the other hand, strains exhibiting an activated cAMP pathway due to a dominant-active allele of *gpa3* display a glossy colony phenotype and are unable to proliferate in plant tumors. Here we present the identification of *sql2* as a suppressor of the glossy colony phenotype of a *gpa3*_{Q206L} strain. *sql2* encodes a protein with similarity to CDC25-like guanine nucleotide exchange factors, which are known to act on Ras proteins. Overexpression of *sql2* leads to filamentous growth that cannot be suppressed by exogenous cAMP, suggesting that *Sql2* does not act upstream of Uac1. To gain more insight in signaling processes regulated by *Sql2*, we isolated two genes encoding Ras proteins. Expression of dominant active alleles of *ras1* and *ras2* showed that *Ras2* induces filamentous growth while *Ras1* does not affect cell morphology but elevates pheromone gene expression. These results indicate that *Ras1* and *Ras2* fulfill different functions in *U. maydis*. Moreover, observed similarities between the filaments induced by *sql2* and *ras2* suggest that *Sql2* is an activator of *Ras2*. Interestingly, *sql2* deletion mutants are affected in pathogenic development but not in mating, indicating a specific function of *sql2* during pathogenesis.

Corn smut disease is caused by the fungal pathogen *Ustilago maydis*. The most prominent symptom of this disease is the formation of large plant tumors (18). The fungal mycelium proliferates within these tumors and finally differentiates into diploid spores (5). In *U. maydis*, pathogenic and sexual development are intimately connected. Fusion of two nonpathogenic haploid cells and subsequent development of the filamentous dikaryon are compulsory for pathogenesis (33). These processes are under the control of two mating-type loci termed *a* and *b*. Cell-cell recognition and fusion are controlled by the *a* locus carrying the pheromone (*mfa*) and receptor (*pra*) genes, while the switch to filamentous growth and all following developmental steps depend on the *b* locus (4, 11). The *b* locus codes for two unrelated homeodomain proteins (bE and bW), which form an active transcription factor only when they are derived from different alleles (27, 36). When haploid strains differ in their *a* and *b* mating-type alleles, they are termed compatible; i.e., they can fuse and undergo sexual and pathogenic development.

During the development of *U. maydis*, the transcription of genes in the *a* and *b* loci is coregulated; prior to fusion, pheromone secreted by haploid cells induces the transcription of the *a* and *b* genes in a compatible partner; after fusion, an autocrine pheromone stimulus triggers the expression of the

active b heterodimer (64). The pheromone-induced transcription, as well as the basal transcription of the *a* and *b* genes, is mediated by the HMG domain transcription factor Prf1 (30). Prf1 is presumed to be activated by the Kpp2/Ubc3 MAP kinase module as well as the cAMP pathway, and both pathways are involved in the regulation of pheromone-responsive gene expression (40, 49). Interestingly, both signaling cascades also influence cell morphology, but they do so in opposing manners. While the mitogen-activated protein kinase (MAPK) module positively regulates filamentous growth, cAMP signaling triggers budding growth. The core components of the MAPK cascade (Kpp2/Ubc3, Fuz7, and Kpp4/Ubc4) (3, 6, 46, 49; P. Müller et al., submitted for publication), as well as of the cAMP cascade, have been characterized. An unknown signal initiates cAMP signaling by activating adenylyl cyclase Uac1, which produces the second messenger cAMP (7). Increasing concentrations of cAMP activate the cAMP-dependent protein kinase (PKA) composed of the regulatory subunit Ubc1 and the catalytic subunit Adr1 (23, 29). Strains disrupted in *uac1* or *adr1* grow filamentously, whereas strains exhibiting constitutively active PKA caused by the deletion of *ubc1* show a cytokinesis defect termed multiple budding (7, 23, 29). Since all these mutants are nonpathogenic, regulated PKA activity appears to be crucial for pathogenic development.

In recent years, it has become evident that cAMP signaling plays a key role during development and pathogenesis in a variety of pathogenic fungi (22). Thus, detailed insight into the regulation of adenylyl cyclases is expected to improve a general understanding of the signaling mechanisms linking development and pathogenicity. In *Saccharomyces cerevisiae*, adenylyl cyclase Cyr1p is regulated by two small G-proteins, Ras1p and Ras2p (37, 61). In addition to Ras, the α -subunit Gpa2p

* Corresponding author. Mailing address: Max Planck Institute for Terrestrial Microbiology, Karl-von-Frisch-Str., D-35043 Marburg, Germany. Phone: 496421178501. Fax: 496421178509. E-mail: Kahmann@mailer.uni-marburg.de.

† Present address: Institute for Toxicology and Genetics, Karlsruhe Research Center, D-76021 Karlsruhe, Germany.

‡ Present address: European Patent Office, D-80331 Munich, Germany.

plays the central roles in activating Cyr1p after the action of glucose stimuli (35, 50). In *U. maydis*, adenylyl cyclase appears to be positively regulated by the G-protein α -subunit Gpa3 (30). Strains expressing a dominant-active allele of *gpa3*, which codes for a α -subunit with strongly reduced GTPase activity, show elevated pheromone gene expression but exhibit an unaltered cell morphology (54). In addition, such strains are able to induce tumors in plants, but they do not proliferate inside the plant tissue (41). Another characteristic phenotype of *gpa3*_{Q206L} strains is a glossy colony phenotype (41). Previously, we isolated suppressors of the glossy colony phenotype of *gpa3*_{Q206L} strains. One of the identified genes was *sql1*, coding for a tetratricopeptide-repeat-type repressor related to Ssn6p of *S. cerevisiae* (44). Overexpression of *sql1* triggered filamentous growth in wild-type cells, presumably by interfering with cAMP signaling on the transcriptional level (44). In this report we describe the characterization of a second gene, *sql2*, identified in the same screen. *sql2* encodes a protein with similarities to guanine nucleotide exchange factors (GEFs) of the CDC25-family. Since Ras proteins are the main effectors of CDC25-like proteins, we have also cloned the genes *ras1* and *ras2* and have analyzed the phenotype of strains expressing dominant-active alleles of either *ras1* or *ras2*.

MATERIALS AND METHODS

Strains and strain constructions. For cloning purposes, the *Escherichia coli* K-12 derivative DH5 α was used. *U. maydis* strains FB1 (*a1b1*), FB2 (*a2b2*), FBD11 (*a1a2b1b2*), FB1gpa3_{OL} and FB2gpa3_{OL} have been described previously (4, 54). FB1P_{crg1}-fuz7DD has been described (Müller et al., submitted). Strains FB1 Δ sql2 and FB2 Δ sql2 were generated by transformation of the wild-type strains with plasmid p Δ sql2 that had been digested with *DraI*. FB1P_{O_{TEF}}:sql2, FB2P_{O_{TEF}}:sql2, FB1gpa3_{OL}P_{O_{TEF}}:sql2, and FB2gpa3_{OL}P_{O_{TEF}}:sql2 were created by transforming the respective progenitor strains with plasmid pOTEF:sql2 that had been digested with *DraI*. In all cases, homologous integration was verified by Southern analysis. FB1P_{crg1}:ras1_{Q67L} was created by transformation of FB1 with pRU11ras1Q67L digested with *SspI*. Single homologous integration into the *ip* locus was verified by Southern analysis as described previously (44). FB2 Δ sql2[pNEBUC] and FB2 Δ sql2[pNEBUC-sql2] were generated by transformation of FB2 Δ sql2 with plasmids pNEBUC and pNEBUC-sql2, respectively, which had been digested with *SspI* prior to transformation. Single ectopic integration events were confirmed by Southern analysis.

To generate FB2ras2_{Q65L} strains, we transformed FB2 with plasmid pRas2Q65L cut with *DraI*. Among 48 transformants screened, we were unable to identify transformants showing homologous integration of the construct. Therefore, we continued to work with three independent transformants harboring single ectopic integrations at different sites in the genome.

Growth conditions for *U. maydis*. *U. maydis* strains were grown as described previously (15). To assay the effects of cAMP on morphology, strains were grown in potato dextrose (PD) liquid medium and on charcoal-containing PD plates to which cAMP was added at the concentrations indicated in the descriptions of the respective experiments. For induction of the *crg1* promoter, strains were grown in complete medium containing 1% glucose to an optical density at 600 nm of 0.8, washed twice in water, and resuspended in complete medium containing 1% arabinose. Hygromycin B was purchased from Roche, phleomycin was purchased from Cayla, and carboxin was purchased from Riedel de Haën. cAMP was added directly to the medium, which was filter sterilized before use. All other chemicals were of analytical grade and were obtained from Sigma or Merck.

The mating reaction was observed by cospotting strains onto charcoal-containing PD plates after incubation at 24°C for 48 h. Plant infections of the corn variety Early Golden Bantam were performed as described previously (49).

Isolation of *sql2*, *ras1*, and *ras2*. To screen for suppressors of FB1gpa3_{OL} the pCM54 library was used as described previously (44). Plasmid pSQL2 harboring an 8-kb fragment containing the entire open reading frame (ORF) of *sql2* and approximately 1.7-kb 5' as well as 3' sequences was isolated. The entire insert was sequenced. With primer combinations ras1f (TACCATTGAGGACTCT TACC) plus ras1r (CGGCAGTATCCAACACATC) and ras2f (ACCATTGAA GACTCGTATCG) plus ras2r (CGCCGGTGTCCAACAGTAC), we amplified

PCR fragments for *ras1* and *ras2*, respectively. We used these fragments for hybridization to filters of a cosmid library (10). From the respective cosmids, we cloned a 3.5-kb *EcoRI* genomic fragment encompassing the *ras1* gene as well as a 3.8-kb *EcoRI* fragment harboring the *ras2* fragment into pTZ18R to obtain pRAS1E and pRAS2E, respectively. To detect the putative intron in *ras1*, we amplified the respective ORF with primers Ras1-5/2 (GATACAAAGTAA CATCGACC) plus Ras1-3/1 (TCTAATGCTGGACAAGGTCG), with cDNA derived from FBD12 as template. The PCR-fragment was cloned into pCR2.1-TOPO and sequenced.

Plasmids and plasmid constructions. Plasmids pTZ19R, pTZ18R (Pharmacia), pBS(-)SKII (Stratagene), and pCR2.1TOPO (Invitrogen) were used for cloning, subcloning, and sequencing. p Δ sql2 is a pBS(-)SKII derivative in which three fragments were ligated into *PstI* and *KpnI* sites. The first 1-kb *NsiI-SspI* fragment (the 5' part of *sql2*) and the second 1.8-kb *HindIII-KpnI* fragment (the 3' part of *sql2*) were isolated from pSQL2. As the third fragment, we used a 2.8-kb *SspI-HindIII* fragment from pSLHyg(-) (15) containing the hygromycin resistance gene. To obtain pOTEF:sql2, we constructed pNEBUC-sql2 by cloning a 6.7-kb *MscI-PfIMI* (blunt) fragment of pSQL2 encompassing the entire ORF of *sql2* into the *PmeI* site of pNEBUC (G. Weinzierl et al., submitted for publication). The resulting plasmid, pNEBUC-sql2, was digested with *BamHI* and *BglII* and subsequently ligated with the *otef* promoter derived as a 0.8-kb *BamHI-BamHI* fragment from pCU4 (44), resulting in pNEBUC-O_{TEF}:sql2. To insert the 5' region of *sql2* and the hygromycin resistance cassette, we performed a three-fragment ligation: the 5' region of *sql2* on a 1.1-kb *BamHI-AgeI* fragment from p Δ sql2 and the hygromycin resistance cassette, isolated as a 2.9-kb *XmaI-BamHI* fragment from pNEBHyg(-) Δ Eco (G. Weinzierl and R. Kahmann, unpublished data), were ligated into *BamHI*-cleaved pNEBUC-O_{TEF}:sql2. From the resulting plasmid, we isolated a 6.2-kb *EcoRI-NsiI* fragment encompassing the 5' region of *sql2*, the hygromycin resistance cassette, the *otef* promoter, and the ORF of *sql2* up to bp +1183 and cloned it into *EcoRI-PstI*-digested pTZ19R. The resulting plasmid was termed pOTEF:sql2.

Plasmid pRas2Q65L contains the 5' region, the *ras2*_{Q65L} allele, a hygromycin resistance cassette, as well as the 3' region of *ras2*. To obtain pRas2Q65L, we first used PCR to introduce a mutation into codon 65 (CAGGAG to CTCGAG), leading to an additional *XhoI* site. For this purpose, we performed two PCRs: for the first, we used primers Ras2-5/1 (AGAATTCATATGAGTGGCAAAT GATG) and Ras2-3/3 (CTCGAGACCAGCCGTGTCAAG); for the second, we used primers Ras2-5/-1 (CTCGAGGAGTACACTGCG); and Ras2-3/2 (GATATCGCTTTCAAAGGATATTGC), introducing an *EcoRV* site at the stop codon. Then we amplified the 3' region of *ras2* by PCR with Ras2KO-5/1 (TCGATATCAAGCAAGCCTCAACAG) and RasKO-3/1 (TAGGGAAATC GCGGCCGC). These PCR products were cloned into pCR2.1TOPO to obtain pCRas2QL-I, pCRas2QL-II, and pCRas2-III, and the inserts were checked for correctness by sequencing. Then the 5' fragment of *ras2* was isolated as a 0.9-kb *NspI-HindIII* fragment from pRAS2E, the 5' part of the ORF was obtained as a 177-bp *HindIII-XhoI* fragment from pCRas2QL-I, the 3' part of the ORF was isolated as a 0.4-kb *XhoI-EcoRV* fragment from pCRas2QL-II, and, finally, the 3' fragment of *ras2* was isolated as a 0.5-kb *EcoRV-EcoRI* fragment from pCRas2QL-III. These four fragments were cloned into pTZ18R digested with *EcoRI-SphI*. The resulting plasmid was opened by digestion with *EcoRV* and ligated with a 2.5-kb *NruI-DraI* phleomycin resistance cassette derived from pSLBle(+) (Weinzierl et al., submitted), finally resulting in pRas2Q65L.

Plasmid pRU11ras1Q67L was derived from pRU11, which is a plasmid for *ip*-locus integration. pRU11 harbors the *sgfp* gene under the control of the *crg1* promoter and the *nos*-terminator (15). To obtain pRU11ras1Q67L, we replaced *sgfp* with the *ras1*_{Q67L} allele. To this end, we performed PCRs to introduce the Q67L mutation that leads to an additional *XhoI* site. In the first PCR with Ras1-5'-NdeI (CATATGTCCAAAGCACAAATCTTG) and Ras1-Q65L (GACAGCTGTATTCTCGAGACCAGCTGTATCC), we introduced an *NdeI* site at the ATG and a *XhoI* site at codon 67. The second PCR was performed with RasQLXhoI (CCGCTCGAGGAATACAGCTGTGAGAAGG) and Ras/3'NotI (GCGGCCGCTTAGAGAACGATACATTCTGG), resulting in the amplified 3' part of *ras1*. Both PCR products were cloned into pCR2.1TOPO and sequenced. To obtain pRU11ras1Q67L, these fragments were then isolated as 0.2-kb *NdeI-XhoI* and 0.6-kb *XhoI-NotI* fragments, respectively, and ligated with both 4.7-kb *BglI-NdeI* and 3.2-kb *BglI-NotI* fragments of pRU11 (15).

DNA and RNA procedures. Standard molecular techniques were used (56). Transformation of *U. maydis* was performed as published previously (58). *U. maydis* DNA was isolated by the method described previously (32). RNA from liquid medium was prepared as published previously (40). The following probes were used for Northern analyses: for *sql2*, a 2.4-kb *NcoI-DraI* fragment derived from pNEBUC-sql2; for *cbx*, a 1.9-kb *NotI-NotI* fragment isolated from pNEBUC; a 675-bp *EcoRV* fragment spanning the *mfa1* gene isolated from pUMa1

(64); and for *frb34*, a 1-kb *EcoRI* isolated from the respective pCR2.1-TOPO clone (15). A 5'-end-labeled oligonucleotide complementary to the *U. maydis* 18S rRNA (12) was hybridized as a loading control in Northern analyses. Radioactive labeling was performed with the NEBlot kit (New England Biolabs). A PhosphorImager (Storm 840; Molecular Dynamics) and the program IMAGE-QUANT (Molecular Dynamics) were used for visualization and quantification of radioactive signals. Sequence information was obtained using an ABI 373 automated sequencer. Sequence analysis was performed with standard bioinformatics tools.

Light microscopy. For microscopic observation, we used a Zeiss Axiophot microscope with differential interference contrast optics. The pictures were taken using a charge-coupled device camera (C4742-95; Hamamatsu, Herrsching, Germany). Image processing were done with Image Pro, Adobe Photoshop 6.0, and Canvas^T 6.0 (Deneba Systems). For documentation, colonies were magnified with an Olympus binocular magnifier.

Nucleotide sequence Accession numbers. The sequence data have been submitted to the GenBank database under accession numbers AY149915 for *sql2*, AY149916 for *ras2*, and AY149917 for *ras1*.

RESULTS

Isolation of *sql2* as suppressor of the glossy colony phenotype of a *gpa3_{Q206L}* strain. Plasmid pSQL2 was isolated by its ability to suppress the glossy colony phenotype of a *gpa3_{Q206L}* strain. pSQL2 contained an 8-kb DNA fragment, and the suppressing activity was mapped to the insert (data not shown). Subsequent sequencing revealed a single ORF of 4,323 bp with no indication for introns. This gene was termed *sql2* and encodes a putative protein of 1,441 amino acids. To confirm that *sql2* is a multicopy suppressor of the glossy colony phenotype of a *gpa3_{Q206L}* strain, we placed the gene under the control of the constitutively strong *otef* promoter (59) by replacing the endogenous promoter of *sql2* in FB1*gpa3_{OL}* (*a1b1*) and FB2*gpa3_{OL}* (*a2b2*). In the resulting strains, FB1*gpa3_{OL}P_{OTEF}:sql2* and FB2*gpa3_{OL}P_{OTEF}:sql2*, *sql2* mRNA was approximately threefold more abundant than in the respective progenitor strains (Fig. 1B). In contrast to the glossy progenitor strain, colonies of these strains did not appear glossy on plates (Fig. 1C, upper panel, shown for FB1*gpa3_{OL}P_{OTEF}:sql2*). To analyze the cell morphology, we propagated FB1*gpa3_{OL}P_{OTEF}:sql2* as well as FB1*gpa3_{OL}* in liquid medium. While FB1*gpa3_{OL}* cells were indistinguishable from the wild type, FB1*gpa3_{OL}P_{OTEF}:sql2* formed aggregates of irregularly branched cells and the individual cells appeared elongated and curved (Fig. 1C, lower panel). This indicates that the suppressing effect of *sql2* is associated with a dramatic change in cellular morphology.

Analysis of the deduced amino acid sequence of *sql2* with SMART and CDART (43, 57) revealed that Ssql2 contains a N-terminal SH3 domain (amino acids 88 to 143), known to be involved in protein-protein interactions, and indicated a RasGEFN domain (amino acids 920 to 1055) and a RasGRF_CDC25 domain (amino acids 1134 to 1386) (Fig. 1A) located in the C terminus. The last two domains are characteristic for proteins belonging to the family of GEFs (guanine nucleotide exchange factors). Such proteins promote the loss of bound GDP and the uptake of GTP in small G-proteins, leading to activation (9, 13). On the basis of sequence similarities, GEFs are classified into two families, the CDC24 family and the CDC25 family. While members of the CDC24 family act on Ras-like G-proteins such as Rho, CDC25 family members activate Ras proteins. Ssql2 displayed no similarities to proteins of the CDC24 family but showed significant similarity to CDC25

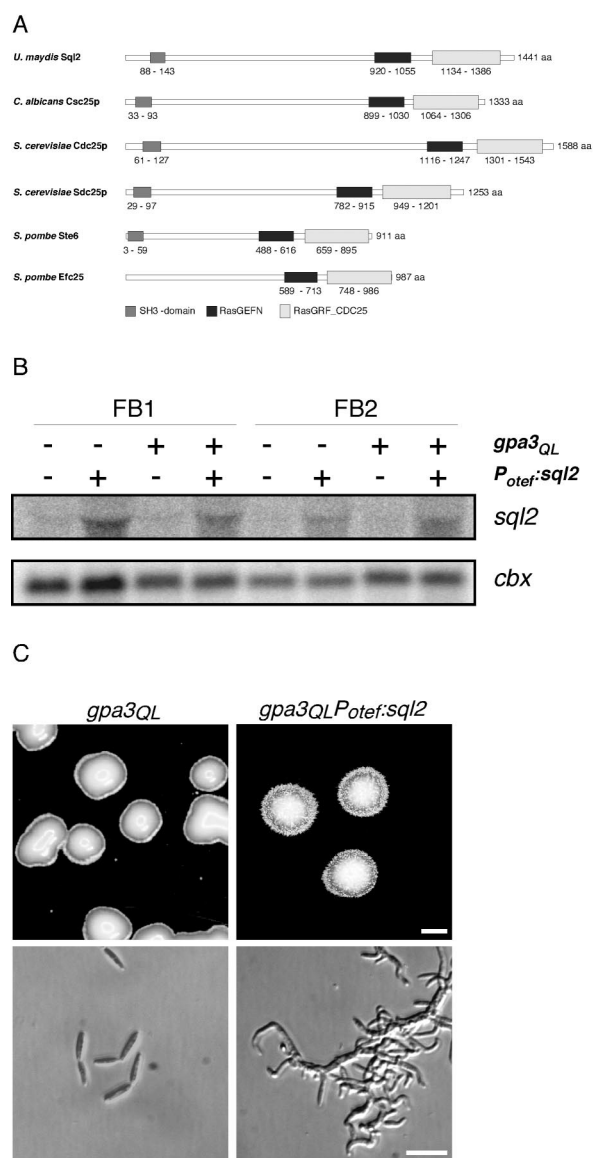


FIG. 1. (A) Domain structure of Ssql2 and its homologues. Domains indicated below were identified using SMART and CDART (<http://smart.embl-heidelberg.de/> and <http://www.ncbi.nlm.nih.gov/Structure/lexington/lexington.cgi?cmd=rps>). Domain annotations: SH3, pfam0001; RasGEFN, smart00229; and RasGRF_CDC25, IPR001895. Numbers represent the amino acid (aa) positions of each domain. Accession numbers: Ssql2, AY149915; Cdc25p, S30356; Cdc25p, CAA27259; Sdc25p, P14771; Ste6, P26674; and Efc25, T40241. (B) Overexpression of *sql2* with the *otef* promoter. Strains indicated at the top were incubated in PD liquid medium; 15 μ g of total RNA was loaded per lane. The same filter was hybridized in succession with probes for *sql2* and *cbx* as loading control. (C) Overexpression of *sql2* suppresses the glossy colony appearance of a *gpa3_{Q206L}* strain. FB1 derivatives indicated at the top were grown on PD-charcoal plates (upper panel) or in PD liquid medium (lower panel). Bars, 1 mm (upper panel) and 20 μ m (lower panel).

family members over its entire length (Cdc25p of *Candida albicans*, 43%; Cdc25p and Sdc25p of *S. cerevisiae*, 40 and 37%, respectively; Ste6 and Efc25 of *Schizosaccharomyces pombe*, 36 and 37%, respectively [Fig. 1A]). Therefore, we conclude that

Sql2 belongs to the CDC25 family of GEFs and might act on Ras proteins in *U. maydis*.

Deletion of *sql2* does not affect mating but interferes with pathogenic development. To analyze the function of *sql2* in more detail, we constructed $\Delta sql2$ deletion strains. To this end, we deleted almost the whole coding region of *sql2* (from positions +22 to +4276) in strains FB1 (*a1b1*) and FB2 (*a2b2*) by replacing this region with a hygromycin resistance cassette (see Materials and Methods). The resulting $\Delta sql2$ deletion strains were viable, showed no apparent growth defect, and displayed a wild-type budding pattern (not shown). Colonies of $\Delta sql2$ deletion mutants exhibited a glossy phenotype, which is similar to *gpa3*_{Q206L} strains, while colonies of the wild-type strain appeared dull (Fig. 2A). It has been shown that the glossy colony phenotype of *gpa3*_{Q206L} strains is correlated with production of an extracellular matrix and does not reflect a special growth mode (41).

The mating ability of $\Delta sql2$ mutants was tested in a plate mating assay, in which the fusion products, the dikaryotic hyphae, appear as white fuzzy filaments (Fig. 2B). Mixtures of compatible $\Delta sql2$ strains developed large numbers of dikaryotic hyphae and in this respect resembled wild-type strains (Fig. 2B). This demonstrated that *sql2* is not necessary for successful recognition, fusion, and filamentous growth.

Interestingly, in the presence of 6 mM cAMP, dikaryon formation of compatible $\Delta sql2$ strains was attenuated, while compatible wild-type strains still formed filaments (Fig. 2C). Moreover, we could hardly detect any dikaryotic filaments in mixtures of compatible $\Delta sql2$ strains when 15 mM cAMP was added to the plates, while under these conditions the wild-type strains showed only a slight reduction of dikaryon formation (Fig. 2B, right panel). It has been demonstrated that high levels of exogenous cAMP (25 mM) inhibit this dimorphic switch (29); however, dikaryon formation of $\Delta sql2$ strains is inhibited by much lower cAMP concentrations. Thus, $\Delta sql2$ strains may be more sensitive to exogenous cAMP, suggesting an influence of *sql2* on the intracellular cAMP content.

To analyze whether *sql2* plays a role during pathogenic development, we infected plants with mixtures of compatible $\Delta sql2$ mutants. Only 10 of 106 infected plants developed tumors (Table 1). This outcome suggests that *sql2* plays an important role during pathogenesis, although it is dispensable for mating. All 10 tumors observed contained fungal spores (data not shown), indicating that lack of *sql2* did not affect fungal development inside the plant tumor. Introduction of the wild-type *sql2* gene into plasmid pNEBUC-*sql2* but not of the empty vector into FB2 $\Delta sql2$ restored pathogenicity (in mixtures with FB1 $\Delta sql2$), demonstrating that the reduction in tumor development was due to deletion of *sql2* (Table 1).

Overexpression of *sql2* does not suppress the proliferation defect of *gpa3*_{Q206L} strains. Compatible strains harboring the *gpa3*_{Q206L} allele are able to induce tumors in corn plants. However, such tumors remain hard and green, most probably due to the observed proliferation defect of *gpa3*_{Q206L} strains (41). Consequently, we wondered whether overexpression of *sql2* would also suppress the proliferation defect of *gpa3*_{Q206L} strains in plant tumor tissue. For this purpose, we infected corn plants with mixtures of FB1*gpa3*_{Q206L}*OTEF::sql2* and FB2*gpa3*_{Q206L}*OTEF::sql2*. Since it has been shown that the *otef* promoter is active in all developmental stages of the fungus, in

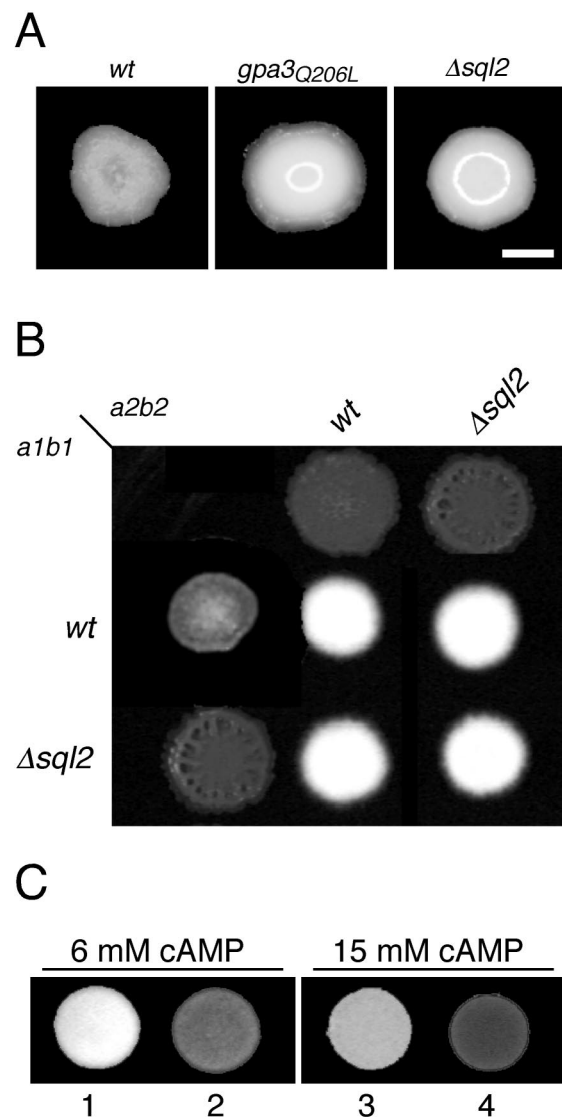


FIG. 2. (A) Deletion of *sql2* leads to a glossy colony appearance. FB1 wild type (*wt*) and derivatives indicated at the top were grown on PD-charcoal plates. Bar, 1 mm. (B) Mating of *sql2* deletion strains. Strains indicated at the top are FB2 (*wt*) and derivatives; strains listed on the left are FB1 (*wt*) and derivatives. Strains were spotted alone or in combinations on PD-charcoal plates and incubated at 24°C for 48 h. (C) Formation of dikaryotic filaments of *sql2* deletion strains is sensitive to cAMP. Mixtures of FB1 and FB2 (1 and 3) and mixtures of FB1 $\Delta sql2$ and FB2 $\Delta sql2$ (2 and 4) were spotted on PD-charcoal plates with 6 mM cAMP (left panel) or 15 mM cAMP (right panel) and incubated at 24°C for 48 h.

the strains used *sql2* should be overexpressed in planta (59). Plant tumors induced by these mixtures resembled tumors induced by compatible *gpa3*_{Q206L} strains (data not shown), demonstrating that overexpression of *sql2* does not suppress the proliferation defect of *gpa3*_{Q206L} strains.

Overexpression of *sql2* induces filamentous growth but does not affect pathogenic growth. Since overexpression of *sql2* in strains harboring *gpa3*_{Q206L} resulted in an altered cell morphology, we have studied the effects of *sql2* overexpression in a wild-type background. To this end, we replaced the endoge-

TABLE 1. Plant infection assays

Inoculum	No. of infected plants	No. of plants with tumors	% Tumor formation
FB1 (<i>alb1</i>) × FB2 (<i>a2b2</i>)	100	72	72
FB1Δ <i>sql2</i> × FB2Δ <i>sql2</i>	106	10	9
FB1P _{OTEF} : <i>sql2</i> × FB2P _{OTEF} : <i>sql2</i>	97	81	83
FB1Δ <i>sql2</i> × FB2	16	10	83
FB1Δ <i>sql2</i> × FB2Δ <i>sql2</i> [pNEBUC]	16	1	6
FB1Δ <i>sql2</i> × FB2Δ <i>sql2</i> [pNEBUC- <i>sql2</i>]#2	15	11	73
FB1Δ <i>sql2</i> × FB2Δ <i>sql2</i> [pNEBUC- <i>sql2</i>]#5	14	10	71

nous *sql2* gene in FB1 by P_{OTEF}:*sql2*, resulting in strain FB1P_{OTEF}:*sql2*. Colonies of FB1P_{OTEF}:*sql2* displayed filamentous growth (Fig. 3A). In liquid media, aggregates of cells were observed, which were elongated and branched (Fig. 3B). This phenotype resembles the filamentous growth of strains with deletion of adenyl cyclase (*Uac1*), which can be made to revert to wild-type morphology by addition of cAMP (28). Interestingly, in the presence of 6 mM cAMP, filament formation of FB1P_{OTEF}:*sql2* on plates was significantly reduced (Fig. 3A), while in liquid medium containing 6 mM cAMP, FB1P_{OTEF}:*sql2* still showed elongated cells (Fig. 3B). However, under these conditions, cell aggregates became denser and filaments were shorter, more branched, and slightly curved (Fig. 3B). These cell aggregates were reminiscent of those observed in FB1gpa3^{QL}P_{OTEF}:*sql2* (Fig. 1B). In the presence of 15 mM cAMP, the wild-type strain FB1 started to grow by multiple budding as described previously (28), while in FB1P_{OTEF}:*sql2*, branching became more prominent and aggregation increased (Fig. 3B). These results show that overexpression of *sql2* in wild-type strains induces filamentous growth, which cannot be made to revert to budding growth by addition of exogenous cAMP.

To analyze whether filamentous growth induced by *sql2* interferes with pathogenic development, we inoculated corn plants with crossings of FB1P_{OTEF}:*sql2* and FB2P_{OTEF}:*sql2*. Interestingly, 83% of infected plants developed tumors, demonstrating that overexpression of *sql2* does not affect pathogenicity (Table 1).

Isolation of two genes encoding Ras homologues. Ras proteins are known to be the main effector proteins of CDC25-like GEFs. Therefore, it was plausible that overexpression or deletion of *sql2* could influence the activity of Ras proteins. To further elucidate the role of *Sql2* in *U. maydis*, we decided to isolate genes coding for Ras proteins.

Using two different short sequence tags showing homology to *ras* genes (kindly provided by Peter Margolis, Versicor, Inc., Fremont, Calif.), we cloned the *ras1* and *ras2* genes of *U. maydis* (see Materials and Methods). Sequencing of the obtained *ras1* clone revealed that the ORF of *ras1* was interrupted by a putative intron of 149 bp. Reverse transcription-PCR analysis confirmed the presence of this intron (data not shown). The *ras1* mRNA codes for a putative protein of 215 amino acids. Sequence analysis of the *ras2* clone indicated that the *ras2* ORF was not disrupted by introns and codes for a putative protein of 192 amino acids. BlastX (2) analysis of *ras1* and *ras2* confirmed that both genes code for proteins with significant homology to other fungal Ras proteins. The deduced proteins have 48% overall identity, which is most prom-

inent in their N-terminal domains. With respect to other fungal Ras proteins, *U. maydis* Ras1 shows high identity to Ras1 proteins from other organisms, e.g., 79% identity to Ras1 of *S. pombe*, 77% identity to Ras1 of *Cryptococcus neoformans*, and 75% identity to Ras1p of *S. cerevisiae*. Ras2 has moderate identity to other Ras2 proteins; e.g., 65% identity to Ras-2 of *Neurospora crassa*, 56% identity to Ras2p of *S. cerevisiae*, and 51% identity to Ras2 of *C. neoformans*. Ras1 and Ras2 from *U. maydis* have a conserved GTP-binding site and a C-terminal CAAX motif commonly found in small GTP-binding proteins.

The dominant-active allele of *ras2* triggers filament formation. To analyze the role of Ras2 in cell morphology, we constructed dominant-active alleles of *ras2* by introducing a point mutation leading to the amino acid substitution Q65L (see Materials and Methods). It was shown that this kind of substitution causes the loss of intrinsic GTPase activity and results in a dominant-active Ras protein (66). To express *ras2*_{Q65L} in *U. maydis*, we introduced this allele under the control of the native promoter into wild-type strain FB2 (see Materials and Methods). We selected three independent transformants that carried one copy of the construct at different sites in the genome (data not shown). All three FB2*ras2*_{Q65L} mutants displayed filamentous growth on plates as well as in liquid media and were indistinguishable from each other (Fig. 3, shown for FB2*ras2*_{Q65L}#5), indicating that this phenotype was due to the dominant-active allele of *ras2*. Filament formation of FB2*ras2*_{Q65L} was strongly reduced when cAMP was added at a final concentration of 6 mM (Fig. 3A). In the presence of 15 mM cAMP, colonies of FB2*ras2*_{Q65L} appeared glossy on the plates (Fig. 3A). In liquid medium, 6 mM cAMP induced branching and curving in filaments induced by *ras2*_{Q65L} (Fig. 3B). In liquid medium containing 15 mM cAMP, FB2*ras2*_{Q65L} cells formed clusters of branched filaments (Fig. 3B). Thus, the morphology of FB2*ras2*_{Q65L} resembled the phenotype of FB1P_{OTEF}:*sql2* (Fig. 3B). However, while both strains responded to exogenous cAMP, the amount of cAMP needed to induce the transitions was different: single colonies of FB2*ras2*_{Q65L} appeared like doughnuts in the presence of 6 mM cAMP, while FB1P_{OTEF}:*sql2* cells formed colonies of this type only with 15 mM cAMP added (Fig. 3A). In addition, exogenous cAMP (15 mM) induced the glossy colony phenotype in FB2*ras2*_{Q65L} but did not do so in FB1P_{OTEF}:*sql2* (Fig. 3A). These differences could be explained by assuming that expression of the dominant-active allele leads to higher levels of active Ras2 compared to active Ras2 levels attained by *sql2* overexpression. On these grounds, we suggest that *Sql2* might be the GEF that activates Ras2.

The dominant-active allele of *ras1* induces *mfa1* gene transcription. To analyze the function of Ras1 in cell morphology, we constructed a dominant-active allele of *ras1* by analogy to the *ras2*_{Q65L} allele. This *ras1*_{Q67L} allele was placed under the control of the *crg1* promoter and introduced into the *ip* locus of FB1 in single copy (12). The *crg1* promoter is repressed by glucose and induced by arabinose. In glucose-containing media, the resulting strain, FB1P_{crg1}:*ras1*_{Q67L}, showed wild-type morphology (data not shown). After a shift to arabinose-containing medium, no morphological changes in FB1P_{crg1}:*ras1*_{Q67L} were observed even after incubation for up to 16 h (data not shown). The absence of an influence on cell morphology suggests that Ras1 is not an effector of *Sql2*.

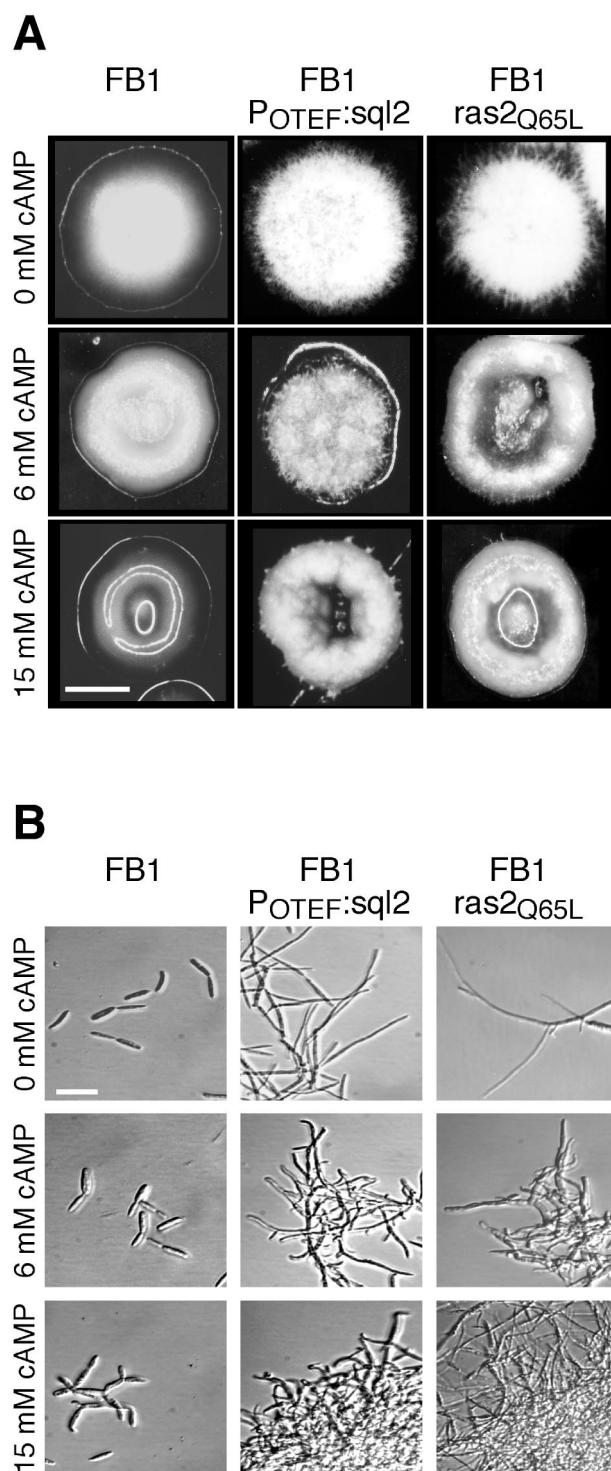


FIG. 3. Overexpression of *sql2* and dominant-active *ras2_{Q65L}* induces filamentous growth. (A) Strains indicated at the top were grown on PD-charcoal plates with 0 mM cAMP (top panel), 6 mM cAMP (middle panel), or 15 mM cAMP (bottom panel). Bar, 1 mm. (B) Strains indicated at the top were grown in PD liquid medium with 0 mM cAMP (top panel), 6 mM cAMP (middle panel) or 15 mM cAMP (bottom panel). Bar, 20 μ m.

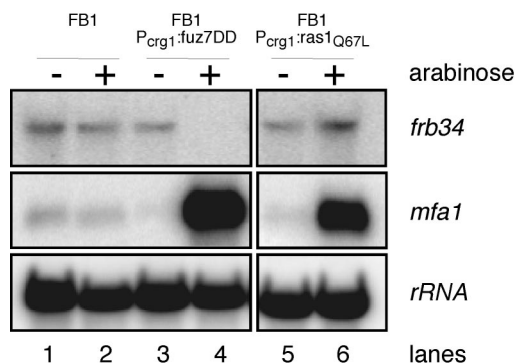


FIG. 4. Dominant-active *ras1_{Q67L}* elevates pheromone gene expression. Strains indicated at the top were incubated in CM containing glucose (-) and then for 5 h in arabinose (+) as the carbon source. A 15- μ g portion of total RNA was loaded per lane. The same filter was hybridized in succession with probes for *mfa1*, *frb34*, and rRNA as the loading control.

Since Ras proteins are known to regulate signaling pathways by interacting with proteins, which contains a so-called Ras association (RA) domain, we searched for proteins containing a putative RA domain. By this computer algorithm-based search, we identified at least three known proteins: the adenylyl cyclase Uac1 (amino acids 970 to 1050), the MAPKK kinase (MAPKKK) kinase Ubc4 (amino acids 44 to 153), and the adaptor protein Ubc2 (amino acids 402 to 490), which most probably acts upstream of Ubc4 (47). Since the cAMP cascade and the MAPK cascade both regulate pheromone gene (*mfa1*) expression, we analyzed whether expression of the *ras1_{Q67L}* allele affects the level of *mfa1* transcription. After inducing the expression of *ras1_{Q67L}*, we detected elevated levels of *mfa1* mRNAs (Fig. 4, lanes 5 and 6), whereas in the progenitor strain FB1, the levels of *mfa1* transcription were unaffected by growth in arabinose-containing medium (lanes 1 and 2). Since *mfa1* transcription is induced by activated cAMP as well as MAPK signaling (40; Müller et al., submitted), we analyzed whether the increased *mfa1* expression triggered by *ras1_{Q67L}* is due to activation of the cAMP cascade or the MAPK module. For this purpose, we chose a second reporter gene, *frb34*, encoding a putative acyltransferase, whose transcription is slightly elevated in the presence of high intracellular cAMP conditions (15). To analyze how this gene responds to an activated MAPK module, we used a strain that expresses a constitutively active allele of the MAPKK gene *fuz7* (*fuz7DD*), under control of the *crg1* promoter. After induction of *fuz7DD*, *frb34* transcription was repressed (Fig. 4, lanes 3 and 4), whereas in the progenitor strain FB1, the expression of *frb34* was not affected by the shift from glucose- to arabinose-containing medium (lanes 1 and 2). Thus, *frb34* is a suitable reporter to distinguish between an active cAMP or MAPK cascade. When *frb34* mRNA levels were compared after induction of *ras1_{Q67L}*, a twofold increase was detected (lanes 5 and 6). Thus, *ras1_{Q67L}* presumably activates the cAMP-signaling cascade to regulate *mfa1* and *frb34* gene expression.

DISCUSSION

In this study, we identified *sql2* as a multicopy suppressor of the glossy colony phenotype of a *gpa3_{Q206L}* strain, which is

supposed to have an activated cAMP pathway. *sql2* encodes a structural homologue of CDC25-like GEFs. In particular, the C-terminal region of *Sql2* contains one RasGEFN domain and RasGRF_CDC25 domain, which are known to catalyze the guanine nucleotide exchange in small G-proteins called Ras proteins (9, 13). In *S. pombe*, two different CDC25-like GEFs, *Ste6* and *Efc25*, are present and have different functions. Deletion of *ste6* abolishes conjugation, while deletion of *efc25* affects cell morphology (34, 62). As in *S. pombe*, the CDC25 homologue of *C. albicans* is not essential for growth but is needed for the dimorphic switch in response to serum (24). In *S. cerevisiae*, two related CDC25-like GEFs exist: *Cdc25p* and *Sdc25p*, both of which have Ras GDP-GTP exchange activity (14, 20). While deletion of *SDC25* results in no obvious phenotype, *CDC25* is essential for growth by acting upstream of *Ras1p* and *Ras2p* (21, 38, 55, 60). In *S. cerevisiae*, *cdc25* strains are viable when exogenous cAMP is provided, which demonstrates that death of *cdc25* strains is due to dysfunction of the adenylyl cyclase *Cyr1p* (17).

In *U. maydis*, the *Cdc25p* homologue *Sql2* differs in function from its homologues *Cdc25p* of *S. cerevisiae* and *Ste6* of *S. pombe* in being dispensable for vegetative growth and conjugation. Δ *sql2* strains show no defect in plate mating assays, demonstrating that *sql2* is not necessary for cell fusion and subsequent development of dikaryotic hyphae. However, *Sql2* is required for full virulence, indicating that it is specifically involved in signaling processes activated during pathogenic development of *U. maydis*.

What are the signaling processes mediated by *Sql2*? The findings that overexpression of *sql2* suppresses the glossy colony appearance of *gpa3*_{Q206L} strains and, conversely, that deletion of *sql2* results in a glossy colony phenotype suggest that *Sql2* influences cAMP signaling negatively. In addition, dikaryon development of Δ *sql2* mutants is more sensitive to cAMP than is that of the wild type. Consistent with a negative effect on cAMP signaling, *sql2* overexpression triggers filamentous growth in haploid strains, which is also observed in strains affected in cAMP signaling. These results suggest that *Sql2* could inhibit cAMP signaling directly. However, we consider it more likely that *Sql2* acts in a pathway that operates in parallel to cAMP signaling. First, suppression of the glossy colony appearance of *gpa3*_{Q206L} strains by *sql2* is associated with a dramatic change in cell morphology, and overexpression of *sql2* fails to suppress the characteristic tumor phenotype of *gpa3*_{Q206L} strains. Thus, in the strict sense, *sql2* cannot be classified as a genuine suppressor, which should have caused the mutant phenotype to revert to the wild type. Second, overexpression of *sql2* does not interfere with pathogenic development, while strains affected in cAMP signaling are nonpathogenic (23). Third, the filamentous phenotype induced by *sql2* is affected by adding cAMP but cannot be made to revert to the budding phenotype seen in wild-type strains. We take this to indicate that *sql2* regulates morphology independently of the cAMP pathway, most probably via a pathway that is interconnected.

CDC25-like GEFs are known to activate Ras proteins by catalyzing the GDP-GTP exchange in these proteins. In this study, we isolated two related genes, *ras1* and *ras2* (48% identity at the amino acid level), encoding proteins that are similar to known fungal Ras proteins. In *U. maydis*, the mRNA levels of

ras1 and *ras2* are comparable (data not shown). Two different Ras genes also exist in *S. cerevisiae*, both of which serve overlapping as well as distinct functions. In yeast, *Ras2p* and *Ras1p* function upstream of the adenylyl cyclase and only *Ras2p* also acts on the STE20/STE11/STE7/KSS1-MAPK module to regulate pseudohyphal differentiation (26, 48, 53). In *S. pombe*, *Ras1* activates the pheromone-responsive MAPK cascade during conjugation and also regulates cell morphology independently of the MAPK cascade (25, 67). Recent studies revealed that these dual roles of *Ras1* are controlled mainly by the action of two different *Cdc25*-like GEFs, *Ste6* and *Efc25*. While *Ste6* couples *Ras1* to the MAPK pathway, *Efc25* links *Ras1* to the *Cdc42* pathway (52). In *U. maydis*, the two different Ras proteins seem to operate in different signaling pathways. Expression of a dominant-active allele of *ras2* induces filaments, while expression of a dominant-active allele of *ras1* does not affect cell morphology but induces pheromone gene expression. In contrast to an activated MAPK module which represses the expression of *fib34*, this reporter gene is induced twofold by *ras1*_{Q67L}. We take this as an indication that *Ras1* activates the cAMP pathway. It has been shown that in *S. cerevisiae*, dominant-active *Ras2p* activates *Cyr1p* and binds to a RA domain found in the leucine-rich repeats of *Cyr1p* (19, 39, 61). The adenylyl cyclase, *Uac1*, of *U. maydis* also harbors a RA domain (amino acids 970 to 1050), and *Ras1* may be coupled to *Uac1* by interaction via this domain.

The second Ras protein in *U. maydis*, *Ras2*, is unlikely to act on adenylyl cyclase, since the filaments developed by strains expressing *ras2*_{Q65L} are clearly distinct from the filaments induced under low-cAMP conditions. In addition, the filaments induced by *ras2*_{Q65L} are similar to the filaments triggered by overexpression of *sql2*. Therefore, we assume that *Sql2* may be the activator of *Ras2*. Consistently, yeast two-hybrid studies show that *Sql2* interacts weakly with *Ras2* but fails to interact with *Ras1* (J. Katzenberger and R. Kahmann, unpublished data). Therefore, it is conceivable that *Ras1* is activated by another, not yet identified, GEF.

The signaling cascade by which *Sql2* and *Ras2* regulate cell morphology in *U. maydis* is not known. One candidate effector pathway may include a *Cdc42* homologue. In *S. pombe*, *Cdc42* is regulated by *Ras1* and acts on the *Pak1/Shk1* kinase involved in polarized growth, presumably by affecting the cytoskeleton. In particular, it was shown that overexpression of dominant-negative *Pak1* results in delocalized actin (51). These and other examples suggest a direct link between Ras signaling and the cytoskeleton in fungi (1, 16, 31, 65) that is critical for morphogenesis. Hence, for the situation in *U. maydis*, it is conceivable that *Sql2* and *Ras2* take part in controlling morphogenesis by regulating the cytoskeleton.

Alternatively, *Ras2* in *U. maydis* may act on the MAPK cascade composed of *Ubc4*, *Fuz7*, and *Kpp2/Ubc3*, since this cascade is a positive regulator of filamentous growth. Moreover, the farthest-upstream component, *Kpp4/Ubc4*, contains a RA domain that is conserved in proteins interacting with Ras proteins (3; Müller et al., submitted). In *S. pombe*, *Ras1* regulates the *Ubc4* homologue, *Byr2*, by interacting with the RA domain of *Byr2* MAPKK kinase, and this interaction leads to the translocation of *Byr2* to the plasma membrane (8, 45, 63). Recently, the *ras2* gene of *U. maydis* was found to act upstream of *kpp2/ubc3* (42). Mutants lacking *ras2* are attenuated in mat-

ing and impaired in pathogenic development (42). To reconcile this with our data that deletion of *sql2* affects pathogenicity only, one would have to propose that *Sql2* might control *Ras2* activity specifically during pathogenic development. For future studies, it will be very interesting to elucidate which signals are transmitted to *Sql2* and to determine how and at which stage *Ras2* becomes activated by *Sql2* or other effectors.

ACKNOWLEDGMENTS

P. Müller and J. Katzenberger contributed equally to the work.

We are most grateful to Peter Margolis (Versicor, Inc., Fremont, Calif.) for providing the two sequence tags of *ras* genes. We thank Jan Schirawski for his critical comments on the manuscript.

This work was supported by the DFG through SFB369. G.L. was supported by a Marie Curie postdoctoral training grant from the European Commission.

REFERENCES

- Alspaugh, J. A., L. M. Cavallo, J. R. Perfect, and J. Heitman. 2000. RAS1 regulates filamentation, mating and growth at high temperature of *Cryptococcus neoformans*. *Mol. Microbiol.* **36**:352–365.
- Altschul, S. F., W. Gish, W. Miller, E. W. Myers, and D. J. Lipman. 1990. Basic local alignment search tool. *J. Mol. Biol.* **215**:403–410.
- Andrews, D. L., J. D. Egan, M. E. Mayorga, and S. E. Gold. 2000. The *Ustilago maydis* *ubc4* and *ubc5* genes encode members of a MAP kinase cascade required for filamentous growth. *Mol. Plant-Microbe Interact.* **13**:781–786.
- Banuett, F., and I. Herskowitz. 1989. Different *a* alleles are necessary for maintenance of filamentous growth but not for meiosis. *Proc. Natl. Acad. Sci. USA* **86**:5878–5882.
- Banuett, F., and I. Herskowitz. 1996. Discrete developmental stages during teliospore formation in the corn smut fungus, *Ustilago maydis*. *Development* **122**:2965–2976.
- Banuett, F., and I. Herskowitz. 1994. Identification of *fuz7*, a *Ustilago maydis* MEK/MAPKK homolog required for *a*-locus-dependent and -independent steps in the fungal life cycle. *Genes Dev.* **8**:1367–1378.
- Barrett, K. J., S. E. Gold, and J. W. Kronstad. 1993. Identification and complementation of a mutation to constitutive filamentous growth in *Ustilago maydis*. *Mol. Plant-Microbe Interact.* **6**:274–283.
- Bauman, P., Q. C. Cheng, and C. F. Albright. 1998. The *Byr2* kinase translocates to the plasma membrane in a *Ras1*-dependent manner. *Biochem. Biophys. Res. Commun.* **244**:468–474.
- Boguski, M. S., and F. McCormick. 1993. Proteins regulating *Ras* and its relatives. *Nature* **366**:643–654.
- Bolker, M., H. U. Bohnert, K. H. Braun, J. Gori, and R. Kahmann. 1995. Tagging pathogenicity genes in *Ustilago maydis* by restriction enzyme-mediated integration (REMI). *Mol. Gen. Genet.* **248**:547–552.
- Bolker, M., M. Urban, and R. Kahmann. 1992. The *a* mating type locus of *U. maydis* specifies cell signaling components. *Cell* **68**:441–450.
- Bottin, A., J. Kamper, and R. Kahmann. 1996. Isolation of a carbon source-regulated gene from *Ustilago maydis*. *Mol. Gen. Genet.* **253**:342–352.
- Bourne, H. R., D. A. Sanders, and F. McCormick. 1991. The GTPase superfamily: conserved structure and molecular mechanism. *Nature* **349**:117–127.
- Boy-Marcotte, E., A. Buu, C. Soustelle, P. Poulet, A. Parmeggiani, and M. Jacquet. 1993. The C-terminal part of the *CDC25* gene product has Ras-nucleotide exchange activity when present in a chimeric *SDC25*-*CDC25* protein. *Curr. Genet.* **23**:397–401.
- Brachmann, A., G. Weinzierl, J. Kamper, and R. Kahmann. 2001. Identification of genes in the bW/bE regulatory cascade in *Ustilago maydis*. *Mol. Microbiol.* **42**:1047–1063.
- Cali, B. M., T. C. Doyle, D. Botstein, and G. R. Fink. 1998. Multiple functions for actin during filamentous growth of *Saccharomyces cerevisiae*. *Mol. Biol. Cell* **9**:1873–1889.
- Camonis, J. H., M. Kalekine, B. Gondre, H. Garreau, E. Boy-Marcotte, and M. Jacquet. 1986. Characterization, cloning and sequence analysis of the *CDC25* gene which controls the cyclic AMP level of *Saccharomyces cerevisiae*. *EMBO J.* **5**:375–380.
- Christensen, J. J. 1963. Corn smut induced by *Ustilago maydis*. *Am. Phytopathol. Soc. Monogr.* **25**:41.
- Colicelli, J., J. Field, R. Ballester, N. Chester, D. Young, and M. Wigler. 1990. Mutational mapping of RAS-responsive domains of the *Saccharomyces cerevisiae* adenylyl cyclase. *Mol. Cell. Biol.* **10**:2539–2543.
- Crechet, J. B., P. Poulet, M. Y. Mistou, A. Parmeggiani, J. Camonis, E. Boy-Marcotte, F. Damak, and M. Jacquet. 1990. Enhancement of the GDP-GTP exchange of RAS proteins by the carboxyl-terminal domain of *SCD25*. *Science* **248**:866–868.
- Damak, F., E. Boy-Marcotte, D. Le-Roscouet, R. Guilbaud, and M. Jacquet. 1991. *SDC25*, a *CDC25*-like gene which contains a RAS-activating domain and is a dispensable gene of *Saccharomyces cerevisiae*. *Mol. Cell. Biol.* **11**:202–212.
- D'Souza, C. A., and J. Heitman. 2001. Conserved cAMP signaling cascades regulate fungal development and virulence. *FEMS Microbiol. Rev.* **25**:349–364.
- Durrenberger, F., K. Wong, and J. W. Kronstad. 1998. Identification of a cAMP-dependent protein kinase catalytic subunit required for virulence and morphogenesis in *Ustilago maydis*. *Proc. Natl. Acad. Sci. USA* **95**:5684–5689.
- Enloe, B., A. Diamond, and A. P. Mitchell. 2000. A single-transformation gene function test in diploid *Candida albicans*. *J. Bacteriol.* **182**:5730–5736.
- Fukui, Y., T. Kozasa, Y. Kaziro, T. Takeda, and M. Yamamoto. 1986. Role of a *ras* homolog in the life cycle of *Schizosaccharomyces pombe*. *Cell* **44**:329–336.
- Gancedo, J. M. 2001. Control of pseudohyphae formation in *Saccharomyces cerevisiae*. *FEMS Microbiol. Rev.* **25**:107–123.
- Gillissen, B., J. Bergemann, C. Sandmann, B. Schroeder, M. Bolker, and R. Kahmann. 1992. A two-component regulatory system for self/non-self recognition in *Ustilago maydis*. *Cell* **68**:647–657.
- Gold, S., G. Duncan, K. Barrett, and J. Kronstad. 1994. cAMP regulates morphogenesis in the fungal pathogen *Ustilago maydis*. *Genes Dev.* **8**:2805–2816.
- Gold, S. E., S. M. Brogdon, M. E. Mayorga, and J. W. Kronstad. 1997. The *Ustilago maydis* regulatory subunit of a cAMP-dependent protein kinase is required for gall formation in maize. *Plant Cell* **9**:1585–1594.
- Hartmann, H. A., R. Kahmann, and M. Bolker. 1996. The pheromone response factor coordinates filamentous growth and pathogenicity in *Ustilago maydis*. *EMBO J.* **15**:1632–1641.
- Ho, J., and A. Bretscher. 2001. *Ras* regulates the polarity of the yeast actin cytoskeleton through the stress response pathway. *Mol. Biol. Cell* **12**:1541–1555.
- Hoffman, C. S., and F. Winston. 1987. A ten-minute DNA preparation from yeast efficiently releases autonomous plasmids for transformation of *E. coli*. *Gene* **57**:267–272.
- Holliday, R. 1974. *Ustilago maydis*, p. 575–595. In R. C. King (ed.), *Handbook of genetics*, vol. 1. Plenum Press, New York, N.Y.
- Hughes, D. A., Y. Fukui, and M. Yamamoto. 1990. Homologous activators of *ras* in fission and budding yeast. *Nature* **344**:355–357.
- Ishiki, T., N. Mochizuki, T. Maeda, and M. Yamamoto. 1992. Characterization of a fission yeast gene, *gpa2*, that encodes a G alpha subunit involved in the monitoring of nutrition. *Genes Dev.* **6**:2455–2462.
- Kamper, J., M. Reichmann, T. Romeis, M. Bolker, and R. Kahmann. 1995. Multiallelic recognition: nonself-dependent dimerization of the bE and bW homeodomain proteins in *Ustilago maydis*. *Cell* **81**:73–83.
- Kataoka, T., D. Broek, and M. Wigler. 1985. DNA sequence and characterization of a fission yeast gene, *gpa2*, that encodes a G alpha subunit involved in the monitoring of nutrition. *Genes Dev.* **6**:2455–2462.
- Kataoka, T., S. Powers, C. McGill, O. Fasano, J. Strathern, J. Broach, and M. Wigler. 1984. Genetic analysis of yeast *RAS1* and *RAS2* genes. *Cell* **37**:437–445.
- Kido, M., F. Shima, T. Satoh, T. Asato, K. Kariya, and T. Kataoka. 2002. Critical function of the Ras-associating domain as a primary Ras-binding site for regulation of *Saccharomyces cerevisiae* adenylyl cyclase. *J. Biol. Chem.* **277**:3117–3123.
- Kruger, J., G. Loubradou, E. Regenfelder, A. Hartmann, and R. Kahmann. 1998. Crosstalk between cAMP and pheromone signalling pathways in *Ustilago maydis*. *Mol. Gen. Genet.* **260**:193–198.
- Kruger, J., G. Loubradou, G. Wanner, E. Regenfelder, M. Feldbrugge, and R. Kahmann. 2000. Activation of the cAMP pathway in *Ustilago maydis* reduces fungal proliferation and teliospore formation in plant tumors. *Mol. Plant-Microbe Interact.* **13**:1034–1040.
- Lee, N., and J. W. Kronstad. 2002. *ras2* controls morphogenesis, pheromone response, and pathogenicity in the fungal pathogen *Ustilago maydis*. *Eukaryot. Cell* **1**:954–966.
- Letunic, I., L. Goodstadt, N. J. Dickens, T. Doerks, J. Schultz, R. Mott, F. Ciccarelli, R. R. Copley, C. P. Ponting, and P. Bork. 2002. Recent improvements to the SMART domain-based sequence annotation resource. *Nucleic Acids Res.* **30**:242–244.
- Loubradou, G., A. Brachmann, M. Feldbrugge, and R. Kahmann. 2001. A homologue of the transcriptional repressor Ssn6p antagonizes cAMP signaling in *Ustilago maydis*. *Mol. Microbiol.* **40**:719–730.
- Masuda, T., K. Kariya, M. Shinkai, T. Okada, and T. Kataoka. 1995. Protein kinase *Byr2* is a target of *Ras1* in the fission yeast *Schizosaccharomyces pombe*. *J. Biol. Chem.* **270**:1979–1982.
- Mayorga, M. E., and S. E. Gold. 1999. A MAP kinase encoded by the *ubc3* gene of *Ustilago maydis* is required for filamentous growth and full virulence. *Mol. Microbiol.* **34**:485–497.
- Mayorga, M. E., and S. E. Gold. 2001. The *ubc2* gene of *Ustilago maydis* encodes a putative novel adaptor protein required for filamentous growth, pheromone response and virulence. *Mol. Microbiol.* **41**:1365–1379.
- Mosch, H. U., R. L. Roberts, and G. R. Fink. 1996. *Ras2* signals via the Cdc42/Ste20/mitogen-activated protein kinase module to induce filamentous

- growth in *Saccharomyces cerevisiae*. Proc. Natl. Acad. Sci. USA **93**:5352–5356.
49. Muller, P., C. Aichinger, M. Feldbrugge, and R. Kahmann. 1999. The MAP kinase *kpp2* regulates mating and pathogenic development in *Ustilago maydis*. Mol. Microbiol. **34**:1007–1017.
50. Nakafuku, M., T. Obara, K. Kaibuchi, I. Miyajima, A. Miyajima, H. Itoh, S. Nakamura, K. Arai, K. Matsumoto, and Y. Kaziro. 1988. Isolation of a second yeast *Saccharomyces cerevisiae* gene (GPA2) coding for guanine nucleotide-binding regulatory protein: studies on its structure and possible functions. Proc. Natl. Acad. Sci. USA **85**:1374–1378.
51. Otilie, S., P. J. Miller, D. I. Johnson, C. L. Creasy, M. A. Sells, S. Bagrodia, S. L. Forsburg, and J. Chernoff. 1995. Fission yeast *pak1+* encodes a protein kinase that interacts with Cdc42p and is involved in the control of cell polarity and mating. EMBO J. **14**:5908–5919.
52. Papadaki, P., V. Pizon, B. Onken, and E. C. Chang. 2002. Two ras pathways in fission yeast are differentially regulated by two ras guanine nucleotide exchange factors. Mol. Cell. Biol. **22**:4598–4606.
53. Peter, M., A. M. Neiman, H. O. Park, M. van Lohuizen, and I. Herskowitz. 1996. Functional analysis of the interaction between the small GTP binding protein Cdc42 and the Ste20 protein kinase in yeast. EMBO J. **15**:7046–7059.
54. Regenfelder, E., T. Spellig, A. Hartmann, S. Lauenstein, M. Bolker, and R. Kahmann. 1997. G proteins in *Ustilago maydis*: transmission of multiple signals? EMBO J. **16**:1934–1942.
55. Robinson, L. C., J. B. Gibbs, M. S. Marshall, I. S. Sigal, and K. Tatchell. 1987. CDC25: a component of the RAS-adenylate cyclase pathway in *Saccharomyces cerevisiae*. Science **235**:1218–1221.
56. Sambrook, J., E. F. Fritsch, and T. Maniatis. 1989. Molecular cloning: a laboratory manual, 2nd ed. Cold Spring Harbor Laboratory Press, Cold Spring Harbor, N.Y.
57. Schultz, J., F. Milpetz, P. Bork, and C. P. Ponting. 1998. SMART, a simple modular architecture research tool: identification of signaling domains. Proc. Natl. Acad. Sci. USA **95**:5857–5864.
58. Schulz, B., F. Banuett, M. Dahl, R. Schlesinger, W. Schäfer, T. Martin, I. Herskowitz, and R. Kahmann. 1990. The *b* alleles of *U. maydis*, whose combinations program pathogenic development, code for polypeptides containing a homeodomain-related motif. Cell **60**:295–306.
59. Spellig, T., A. Bottin, and R. Kahmann. 1996. Green fluorescent protein (GFP) as a new vital marker in the phytopathogenic fungus *Ustilago maydis*. Mol. Gen. Genet. **252**:503–509.
60. Tatchell, K., D. T. Chaleff, D. DeFeo-Jones, and E. M. Scolnick. 1984. Requirement of either of a pair of ras-related genes of *Saccharomyces cerevisiae* for spore viability. Nature **309**:523–527.
61. Toda, T., I. Uno, T. Ishikawa, S. Powers, T. Kataoka, D. Broek, S. Cameron, J. Broach, K. Matsumoto, and M. Wigler. 1985. In yeast, RAS proteins are controlling elements of adenylate cyclase. Cell **40**:27–36.
62. Tratner, I., A. Fourticiq-Esqueoute, J. Tillit, and G. Baldacci. 1997. Cloning and characterization of the *S. pombe* gene *efc25+*, a new putative guanine nucleotide exchange factor. Gene **193**:203–210.
63. Tu, H., M. Barr, D. L. Dong, and M. Wigler. 1997. Multiple regulatory domains on the Byr2 protein kinase. Mol. Cell. Biol. **17**:5876–5887.
64. Urban, M., R. Kahmann, and M. Bolker. 1996. Identification of the pheromone response element in *Ustilago maydis*. Mol. Gen. Genet. **251**:31–37.
65. Waugh, M. S., C. B. Nichols, C. M. DeCesare, G. M. Cox, J. Heitman, and J. A. Alspaugh. 2002. Ras1 and Ras2 contribute shared and unique roles in physiology and virulence of *Cryptococcus neoformans*. Microbiology **148**:191–201.
66. Wiseman, R. W., S. J. Stowers, E. C. Miller, M. W. Anderson, and J. A. Miller. 1986. Activating mutations of the *c-Ha-ras* protooncogene in chemically induced hepatomas of the male B6C3 F₁ mouse. Proc. Natl. Acad. Sci. USA **83**:5825–5829.
67. Xu, H. P., M. White, S. Marcus, and M. Wigler. 1994. Concerted action of RAS and G proteins in the sexual response pathways of *Schizosaccharomyces pombe*. Mol. Cell. Biol. **14**:50–58.